Mem. S.A.It. Vol. 95, 12

Memorie della

Preliminary X-ray timing of the accreting millisecond pulsar SAX J1808.4-3658 during the latest stages of the 2022 outburst

C. Ballocco[2,1], A. Papitto[1], A. Miraval Zanon[3,1], and G. Illiano[1,4,2]

[1] Istituto Nazionale di Astrofisica - Osservatorio Astronomico di Roma, via Frascati 33, Monte Porzio Catone (RM), 00078, Italy
[2] Sapienza Università di Roma, Piazzale Aldo Moro 5, I-00185 Rome, Italy
[3] Agenzia Spaziale Italiana, Via del Politecnico snc, I-00133 Rome, Italy
[4] Università degli Studi di Roma "Tor Vergata", Via della Ricerca Scientifica 1, 00133 Rome, Italy
e-mail: caterina.ballocco@inaf.it

Received: 1 December 2023; Accepted: 24 January 2024

Abstract. We report on the preliminary results of the coherent X-ray timing analysis of the accreting millisecond X-ray pulsar SAX J1808.4-3658, using XMM-Newton data acquired during the final stages of the 2022 outburst. We derived an updated orbital solution of the binary system and investigated the evolution of the neutron star spin frequency. A study of the phase delays of the pulse profile reveals a notable evolution in the pulse phase. These observed phase shifts apparently take place simultaneously to X-ray flux variations and suggest an interpretation in terms of drifts of the hot spots on the neutron star surface, influenced by variations in the mass accretion rate.

Key words. stars: neutron - X-rays: binaries - X-rays: individual (SAX J1808.4-3658)

1. Introduction

Millisecond pulsars (MSPs) are neutron stars (NSs) that rotate very rapidly. They are characterized by spin periods of the order of a few milliseconds and magnetic fields of approximately $10^8 - 10^9$ G. Low-mass X-ray binary systems (LMXBs) are believed to be their progenitors. These NSs are in fact assumed to be spun up or "recycled" through accretion of matter and angular momentum from its companion star that has overflowed its Roche lobe (Alpar et al. 1982; Bhattacharya & van den Heuvel 1991). During the accretion phase, the transfer of angular momentum can accelerate the pulsar rotation to hundreds of times per second, as is observed in millisecond pulsars. Accreting Millisecond X-ray Pulsars (AMXPs) are characterized by long quiescence periods (lasting years to decades) interrupted by short outburst phases (lasting weeks to months) during which the X-ray emission increases by orders of magnitude.
SAX J1808.4-3658 (hereafter SAX J1808) is a transient LMXB that was discovered by the X-ray satellite BeppoSAX during an X-ray out-

burst in 1996 (in 't Zand et al. 1998). The detection of X-ray pulsations at $\sim$ 401 Hz with the Rossi X-ray Timing Explorer (RXTE) during the subsequent outburst in 1998 (Wijnands & van der Klis 1998) marked this source as the first accreting millisecond X-ray pulsar. The pulsar rotates with a period of 2.49 ms and orbits around a companion star of approximately 0.04 $M_\odot$ (Bildsten & Chakrabarty 2001) with an orbital period of $\sim$ 2 h (Chakrabarty & Morgan 1998). It is located at a distance of about 3.5 kpc (Galloway & Cumming 2006). Since its discovery, ten outbursts have been observed, each lasting approximately one month, with recurrence intervals of roughly 2-3 years. On 2022 August 19, the onset of a new outburst was detected by the MAXI/GSC nova alert system (Imai et al. 2022), and later confirmed by rapid targeted follow-up NICER observations (Sanna et al. 2022a). SAX J1808 stands out as the most extensively studied among the AMXPs, having displayed the highest number of outbursts. During these outbursts, the X-ray source luminosity typically reaches around 10^{36} erg s^{-1} Gilfanov et al. (1998), starting from a quiescent level of $\sim 5 \times 10^{31}$ erg s^{-1} (Campana et al. 2004).

During the 2019 outburst, SAX J1808 exhibited coherent millisecond optical and UV pulsations (Ambrosino et al. 2021). The luminosity of both optical and UV pulsations is remarkably high ($L_{\rm optical} \approx 3 \times 10^{31}$ erg s^{-1}, $L_{\rm UV} \approx 2 \times 10^{32}$ erg s^{-1}), challenging for current accretion model. Optical and UV pulsations were observed both in the rising phase and in the last part of the outburst. In the latest outburst in 2022, optical pulsations were still detected, this time closer to the peak of the outburst (Miraval Zanon et al. in prep.).

SAX J1808 displays peculiar oscillating states of low luminosity known as "reflares", which occur after the end of the main outburst (Patruno et al. 2016). These reflares are characterized by a sequence of bumps, exhibiting quasi-oscillatory behavior over a few days and a luminosity variation of up to three orders of magnitude on timescales of approximately 1-2 days. The final flaring phase is of particular interest as it provides insights into the physics of the accretion disk at low accretion rates, potentially entering the propeller regime (Patruno et al. 2009b). This flaring tail phenomenon has been consistently observed in all outbursts of SAX J1808, including the 2022 event. For the latter, we conducted an XMM–Newton observation on September 9, 2022 (Obs.ID. 0884700801, PI: A. Papitto).

Here, we present a coherent phase timing analysis performed on XMM-Newton observations acquired during the final phase of the outburst. We aim at determining the orbital parameters of the system and explore the evolution of pulse phases during the reflaring stage.

2. Observations

The XMM-Newton satellite (Jansen et al. 2001) observed SAX J1808 for 125 ks starting on September 9, 2022 at 14:22:09 (UTC). The 0.3-10 keV light curve is displayed in the top panel of Fig. 1. The data were processed and reduced using the Science Analysis System (SAS; v.20.0.0). We converted the photon arrival times observed by XMM-Newton to the Solar System Barycenter using the source position derived by Hartman et al. (2008) and the `barycen` tool, and then to the line of nodes using the the JPL ephemerides DE405.

The EPIC-pn camera operated in timing mode to allow the necessary temporal resolution (29.5 μs) needed to study the millisecond variability of the source and was equipped with thick filter. The EPIC-MOS2 camera observed in timing mode, while EPIC-MOS1 operated in Small Window to provide an image of the source, with time resolution of 1.75 ms and 0.3 s respectively. The effective exposure is reduced to 108.2 ks due to the removed soft proton flaring episodes characterized by an EPIC-pn 10-12 keV count rate exceeding 0.8 c/s. In timing mode, to allow a faster readout the spatial information along one of the optical axis is lost. The maximum number of counts was recorded in pixels characterized by RAWX coordinates 37 and 38. The EPIC-pn spectrum has been extracted considering a 21 pixels wide region (1 pixel $\simeq 4.1''$) around the source position, spanning from RAWX = 28 to 48. The background was estimated far from the source, in a 3 pixel-wide region centered

on RAWX = 4.
During the XMM-Newton pointing SAX J1808 exhibited two Type I X-ray bursts. Type I X-ray bursts are thermonuclear explosions caused by unstable burning of accreted hydrogen or helium on the surface of NSs in LMXB. They manifest as a sudden increase in the X-ray intensity many times brighter than the persistent level (Galloway et al. 2008). When analysing the persistent emission we created good time intervals (GTIs), discarding a time interval starting 10 s before and ending 150 s after each burst onset. No additional evident variability trend was observed over time scales going from a few seconds to the length of the observation.

3. Coherent Timing Analysis

We performed a phase-coherent timing analysis of the 2022 outburst of SAX J1808, using the XMM-Newton/EPIC-pn high-time resolution observation. We first corrected the photon arrival times for the binary Doppler delays based on the ephemeris evaluated by Illiano et al. (2023) using NICER data taken during the outburst from 2022 August 19 (MJD 59810) until 2022 October 5 (MJD 59857). In particular we estimated the time delays caused by the binary motion of the system assuming an almost circular orbit (Burderi et al. 2007; Sanna et al. 2016), through the formula

$$t_{arr} - t_{em} = \frac{a\,sini}{c} sin\left(\frac{2\pi}{P_{orb}}(t - T_{asc})\right), \quad (1)$$

where t_{arr} is the photon arrival time to the Solar System Barycentre, t_{em} is photon emission time, $a\,sini/c$ is the projected semimajor axis of the NS orbit in light seconds, P_{orb} is the orbital period and T_{asc} is the epoch of passage at the ascending node.
To enhance the precision of orbital parameters estimates we used the Epoch Folding Search technique (EFS, Leahy 1987). The EFS involves searching for periodicities in a time series by folding the light curve over a range of different periods, centered around the best estimate available. The statistical measure used to assess the goodness of each individual period is the χ^2 of the folded profile. In our case the periods $P(t)$ are valued by performing an EFS on 1 ks long data segments. The obtained variance profiles are subsequently fitted with a Gaussian, as described by Leahy (1987). The correction of photon arrival times using Eq. 1 introduces a "smearing" effect in a pulse profile derived from an EFS performed on the corrected light curve. This smearing is attributed to corrections influenced by errors in estimating orbital parameters. After obtaining the best period estimate for each time interval and converting them to frequency, we apply a simple differentiation of the Doppler effect formula to fit the frequency variation

$$\begin{aligned}\nu(t) - \nu_0 = \frac{\partial\nu(t)}{\partial\nu_0}\Delta\nu_0 + \frac{\partial\nu(t)}{\partial P_{orb}}\Delta P_{orb} + \\ + \frac{\partial\nu(t)}{\partial\, T_{asc}}\Delta T_{asc} + \frac{\partial\nu(t)}{\partial a\,sini}\Delta a\,sini\,,\end{aligned} \quad (2)$$

where $\Delta\nu_0$, ΔP_{orb}, ΔT_{asc} and $\Delta a\,sini$ are the residual Doppler modulations caused by differences between the actual orbital parameters and those used to correct the photon time of arrivals.
In order to determine a more accurate set of ephemeris and analyze the frequency evolution of the source, we can study variations in the phase of the pulse profile. Phase variation arises from differences between the actual pulsar spin period and the one we use to fold our data. The expected phase variations can be computed by

$$\delta\phi_{\dot\nu} = \int_{T_0}^{t}\Big[\int_{T_0}^{t'}\dot\nu(t'')dt''\Big]dt'. \quad (3)$$

We note that a difference between the real pulsar spin frequency and the folding frequency gives a linear trend in the phases, while a first derivative results in a parabolic trend. Lastly, any remaining orbital modulation induces a sinusoidal trend in the residues at the orbital period (Burderi et al. 2007).
We therefore divided our observation in 1 ks time intervals and folded them around the best estimate of the spin frequency we have ν_F, using 16 phase bins. We modeled each pulse profile by fitting it with a constant and two har-

Table 1. Orbital parameters of SAX J1808 obtained from the timing analysis of the XMM-Newton observations during the reflaring stage of the 2022 outburst. Errors are at 1σ confidence level.

Parameter	Value
Epoch, T_0 (MJD)	59831.7381191
P_{orb} (s)	7249.25(88)
$a \sin i/c$ (lt-s)	0.06289(22)
T_{asc} (MJD)	59810.6183(26)
ν (Hz)	400.97521092(99)
χ^2/d.o.f	1367.3/87

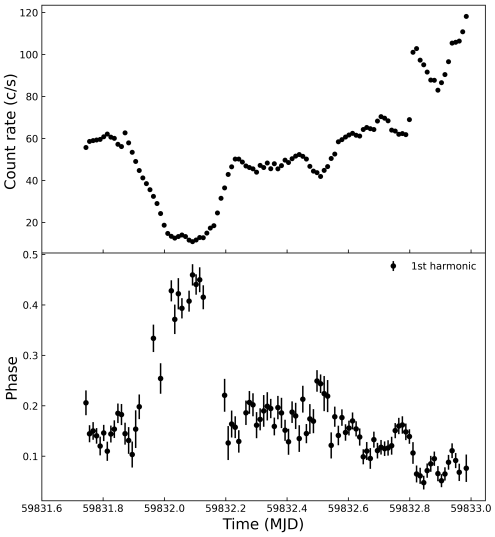

Fig. 1. Top panel: the 0.5-10 keV light curve using 1 ks bins. Lower panel: time evolution of the pulse phase delays for the fundamental computed by folding XMM-Newton observation at the spin frequency $\nu_F = 400.975209557$ Hz.

monic components. We selected only statistically significant pulse profiles, i.e. folded profiles with a ratio between the sinusoidal amplitude and 1σ uncertainty equal to or greater than three. In this way, we obtain the phase delays shown in Fig. 1 for the fundamental. In this work, we focused on the fundamental phase since it is significantly detected more often than the second harmonic.

To proceed further with the analysis, we modeled the time evolution of the pulse phase delays obtained from the fundamental harmonic as follows (Sanna et al. 2022b; Papitto et al. 2007):

$$\phi(t) = \phi_0 - \Delta\nu(t-T_0) - \frac{1}{2}\dot{\nu}(t-T_0)^2 + R_{orb}(t), \quad (4)$$

where ν is the NS spin frequency, T_0 is the reference epoch, $\Delta\nu = \nu(T_0) - \nu_F$ and $\dot{\nu}$ represent the correction factor on the frequency used to epoch-fold the data and the spin frequency derivative, respectively. R_{orb} models the residual orbital modulation due to the differential corrections between the adopted NS orbital parameters and the real ones (Deeter et al. 1981). In Table 1 we reported the best-fitting orbital parameters we obtained. Note that we rescaled the uncertainties of the fit parameters multiplying them by the square root of the reduced χ^2 to take into account the statistical inadequacy of the fit.

4. Discussion and Conclusions

In this work, we present the preliminary coherent timing solution for the AMXP SAX J1808 obtained from the analysis of XMM-Newton observations acquired during the reflaring stage of 2022 outburst. The set of orbital parameters reported in Table 1 is compatible within the errors with the timing solution obtained from NICER observation of the same outburst reported by Illiano et al. (2023). The uncertainties associated with our best-fitting values are higher than those derived from the NICER observation. This discrepancy arises because NICER monitored the entire outburst, spanning approximately 47 days. On the other side, the XMM-Newton observation lasted roughly 1 day, focusing specifically on the reflaring state of the outburst. The value of the spin frequency obtained in this work is not compatible within the errors with that reported in Illiano et al. (2023). This is likely associated with the observed phase noise in the XMM data. Furthermore, as illustrated in Fig. 1, the phase delays display a known phenomenon of

phase shifts, characterized by a distinct jump of approximately 0.4 in phase occurring around 59832 MJD. Notably, in the light curve, this corresponds to a change in the trend of the X-ray source flux (see Fig.1, top panel). The significant variability in the phases of SAX J1808 is a well-known phenomenon, apparent from the existence of unmodeled phase residuals in comparison to the adopted timing solution (Burderi et al. 2006). This significantly restricted the capability to measure the spin evolution of NS through pulse phase timing, thereby explaining the different spin frequency obtained in this work. Patruno et al. (2009a) suggested that a significant fraction of the unmodeled phase variability could be attributed to a correlation between pulse phase and X-ray flux. This phase-flux correlation is interpreted in terms of hot spot drift on the NS surface, driven by changes in the mass accretion rate (Kulkarni & Romanova 2013). To account for the phase shifts, Bult et al. (2020) introduced a phase-flux correlation term related to hot spot drifts by adding a flux-dependent adjustment to our timing model. This model will be properly investigated and applied to the XMM-Newton 2022 outburst observation in a follow-up paper in order to better understand the pulse phase evolution during the reflaring stage of the source.

Acknowledgements. We acknowledge financial support from National Institute for Astrophysics (INAF) Research Grant "Uncovering the optical beat of the fastest magnetised neutron stars (FANS)" and from the Italian Ministry of University and Research (MUR), PRIN 2020 (prot. 2020BRP57Z) "Gravitational and Electromagnetic-wave Sources in the Universe with current and next-generation detectors (GEMS)".

References

Alpar, M. A., Cheng, A. F., Ruderman, M. A., & Shaham, J. 1982, Nature, 300, 728
Ambrosino, F., Miraval Zanon, A., Papitto, A., et al. 2021, Nature Astronomy, 5, 552
Bhattacharya, D. & van den Heuvel, E. P. J. 1991, Phys. Rep., 203, 1
Bildsten, L. & Chakrabarty, D. 2001, ApJ, 557, 292
Bult, P., Chakrabarty, D., Arzoumanian, Z., et al. 2020, ApJ, 898, 38
Burderi, L., Di Salvo, T., Lavagetto, G., et al. 2007, ApJ, 657, 961
Burderi, L., Di Salvo, T., Menna, M. T., Riggio, A., & Papitto, A. 2006, ApJ, 653, L133
Campana, S., D'Avanzo, P., Casares, J., et al. 2004, ApJ, 614, L49
Chakrabarty, D. & Morgan, E. H. 1998, Nature, 394, 346
Deeter, J. E., Boynton, P. E., & Pravdo, S. H. 1981, ApJ, 247, 1003
Galloway, D. K. & Cumming, A. 2006, ApJ, 652, 559
Galloway, D. K., Muno, M. P., Hartman, J. M., Psaltis, D., & Chakrabarty, D. 2008, ApJS, 179, 360
Gilfanov, M., Revnivtsev, M., Sunyaev, R., & Churazov, E. 1998, A&A, 338, L83
Hartman, J. M., Patruno, A., Chakrabarty, D., et al. 2008, ApJ, 675, 1468
Illiano, G., Papitto, A., Sanna, A., et al. 2023, ApJ, 942, L40
Imai, Y., Serino, M., Negoro, H., et al. 2022, The Astronomer's Telegram, 15563, 1
in 't Zand, J. J. M., Heise, J., Muller, J. M., et al. 1998, A&A, 331, L25
Jansen, F., Lumb, D., Altieri, B., et al. 2001, A&A, 365, L1
Kulkarni, A. K. & Romanova, M. M. 2013, MNRAS, 433, 3048
Leahy, D. A. 1987, A&A, 180, 275
Papitto, A., di Salvo, T., Burderi, L., et al. 2007, MNRAS, 375, 971
Patruno, A., Maitra, D., Curran, P. A., et al. 2016, ApJ, 817, 100
Patruno, A., Rea, N., Altamirano, D., et al. 2009a, MNRAS, 396, L51
Patruno, A., Watts, A., Klein Wolt, M., Wijnands, R., & van der Klis, M. 2009b, ApJ, 707, 1296
Sanna, A., Bult, P., Gendreau, K., et al. 2022a, The Astronomer's Telegram, 15559, 1
Sanna, A., Burderi, L., Di Salvo, T., et al. 2022b, MNRAS, 514, 4385
Sanna, A., Burderi, L., Riggio, A., et al. 2016, MNRAS, 459, 1340
Wijnands, R. & van der Klis, M. 1998, Nature, 394, 344